ICAR '97
Monterey, CA, July 7-9, 1997

Design of Non-Redundant Manipulators for Optimal Dynamic Performance

Alan Bowling and Oussama Khatib

Robotics Laboratory
Department of Computer Science
Stanford University, Stanford, CA 94086

Abstract

This article investigates the problem of robotic manipulator design for optimal dynamic performance. We present a design methodology which consolidates some of the major issues related to manipulator dynamic performance. These issues are related to workspace volume, actuator selection, control authority, inertial properties, and acceleration capability. This is accomplished using a new characterization of end effector acceleration properties we recently proposed. Performance measures obtained from this characterization are used within an optimization procedure to determine the design parameters which improve manipulator dynamic performance. The approach is applied to the problem of design parameter selection for a simple three degree-of-freedom planar mechanism.

KEYWORDS: Robot Design, Optimal Dynamics, Acceleration Characteristics, Inertial Properties, Dynamic Performance

1 Introduction

This article presents an optimization procedure which, through the use of newly developed performance measures, consolidates some of the major issues related to dynamic performance. The study of dynamic performance involves issues dealing with how responsive a manipulator is to controller commands. These commands can specify motions to be performed or forces to be applied to the environment. Our studies of dynamic performance center around consideration of the inertial properties as perceived at the end effector and the manipulator's ability to accelerate its end effector. These characteristics are are embodied in the equations of motion which relate inertial properties and accelerations to actuator forces and moments.

A number of studies of manipulator performance have focused on analysis of the manipulator's kinematic properties represented by the Jacobian transformation. These efforts yielded important measures and characterizations related to kinematic properties [1, 12, 14, 20] and static force capability [16]. However, the Jacobian does not contain information about inertial properties and other factors which must be overcome in order to accelerate the end effector.

Other studies directly analyze the end effector inertial properties [2, 8]. However, these properties do not describe the actuator effort needed to produce end effector acceleration. Several efforts were devoted to the analysis of end effector acceleration capability [6, 9, 11, 13, 19, 21]. Most of these studies did not adequately treat the inhomogeneities between properties related to linear and angular motion.

Our work in this area separately considers linear and angular, accelerations and velocities, resulting in a more physically meaningful characterization of acceleration capability, [4, 3]. The use of new performance measures, based on this characterization, has allowed the formulation of an optimization procedure which simultaneously addresses many of the issues related to dynamic performance; specifically with respect to workspace volume, actuator sizing, control authority, inertial properties, and acceleration capability.

We first present the characterization of acceleration capability and the performance measures obtained from it. Synthesis of the characterization and measures into an optimization procedure is then discussed. Finally, the optimization procedure is applied to the problem of design parameter selection for a standard three degree-of-freedom (DOF) planar manipulator.

2 Characterization

The characterization of acceleration capability results from analysis of end effector, isotropic, linear and angular, accelerations and velocities. Here the isotropic acceleration/velocity is defined as the largest magnitude of acceleration/velocity achievable at the end effector, in or about every direction. A brief description of the development of this characterization is given below; for more details see [4, 3].

The analysis begins by considering the bounds on

actuator torque capacity,

$$-\Upsilon_{bound} \leq \Upsilon \leq \Upsilon_{bound}. \quad (1)$$

End effector dynamic behavior is described by,

$$\Lambda \begin{bmatrix} \dot{v} \\ \dot{\omega} \end{bmatrix} + \mu + \mathbf{p} = \mathbf{F} \quad (2)$$

and

$$\Upsilon = \mathcal{T}^{-1} J^T \mathbf{F} \quad (3)$$

where Λ describes the inertial properties as perceived at the end effector and $\dot{v}$ and $\dot{\omega}$ are the end effector linear and angular accelerations. μ, $\mathbf{p}$, $\mathbf{F}$, J, and $\mathcal{T}$ are respectively the centrifugal and Coriolis force vector, gravity force vector, generalized force vector acting in operational space, Jacobian matrix, and transformation between joint torques and actuator torques.

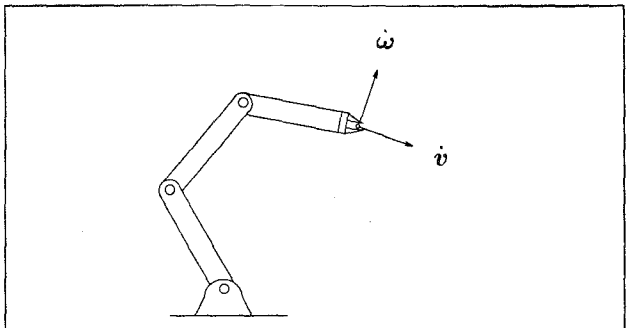

Figure 1: 3 DOF Planar Manipulator.

Using the above equations the following relationship is obtained,

$$\Upsilon_{lower} \leq E_v \dot{v} + E_\omega \dot{\omega} + \bar{\mathbf{b}} \leq \Upsilon_{upper} \quad (4)$$

where

$$[E_v \; E_\omega] = N\mathcal{T}^{-1} J^T \Lambda \qquad \Upsilon_{upper} = \mathbf{1} - N\mathcal{T}^{-1} J^T \mathbf{p}$$
$$\bar{\mathbf{b}} = N\mathcal{T}^{-1} J^T \mu \qquad \Upsilon_{lower} = -\mathbf{1} - N\mathcal{T}^{-1} J^T \mathbf{p}. \quad (5)$$

In obtaining this equation the bounds, Υ_{bound}, have been normalized using a diagonal matrix N with elements $N_{ii} = \frac{1}{\Upsilon_{bound_i}}$.

A set of equations describing the relationships between end effector, isotropic, linear and angular, accelerations and velocities, $||\dot{v}||$, $||\dot{\omega}||$, $||v||$, and $||\omega||$, is then derived from equation (4). This is done by mapping spherical surfaces representing the isotropic quantities through equation (4), yielding,

$$\mathcal{A} \begin{bmatrix} ||\dot{v}|| \\ ||\dot{\omega}|| \end{bmatrix} + \mathcal{C}(||v||, ||\omega||) = \begin{bmatrix} \Upsilon_{upper} \\ \Upsilon_{lower} \end{bmatrix} \quad (6)$$

where $\mathcal{A}$ is a matrix of scalar coefficients and $\mathcal{C}(||v||, ||\omega||)$ is a vector which approximates the effect of linear and angular velocities. Each element of $\mathcal{C}(||v||, ||\omega||)$ is a nonlinear function of $||v||$ and $||\omega||$.

The four-dimensional relationship in equation (6) can be represented as a hypersurface. Its characteristics can only be displayed along different sections cut by particular hyperplanes. An example of this is given in Figure 2 where the sectioning hyperplane is defined as $||\omega|| = 0$. Figure 2 is calculated at one configuration of the mechanism in Figure 1.

The hypersurface describes the bounds on the worst case combinations of linear and angular, accelerations and velocities which saturate one or more actuators. All combinations of acceleration and velocity beneath the hypersurface are achievable in every direction at this configuration. The $\triangle$ in Figure 2 marks the isotropic linear acceleration achievable from rest if the end effector moves without changing its orientation. The $\bigcirc$ marks the isotropic angular acceleration achievable from rest if the end effector rotates without translating a reference point on the end effector. If the end effector moves from rest with some combination of linear and angular motion, the largest combination achievable in every direction is bounded by the curve in the $||\dot{v}|| - ||\dot{\omega}||$ plane.

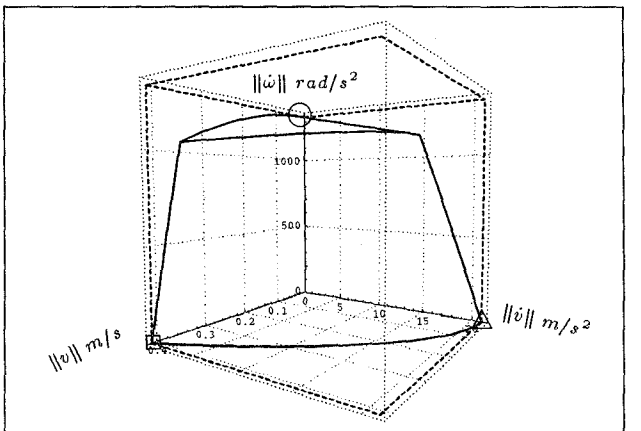

Figure 2: Isotropy Surface.

The remaining portions of the surface show the achievable acceleration from a particular velocity state. End effector velocities can limit performance because the manipulator may have to overcome Coriolis/centrifugal forces in order to move in a desired direction. In the worst case, the $\square$ in Figure 2 marks the condition where, in some direction, there is only enough torque available to compensate for the Coriolis/centrifugal forces and gravity forces, but not enough to obtain an arbitrary desired acceleration.

The hypersurface of Figure 2 describes the manipulator performance at one specific configuration. It

is desirable to describe how acceleration capability changes over the workspace. In order to do this a set of hypersurfaces obtained from different configurations can be statistically analyzed to obtain minimum, maximum, average, and standard deviation hypersurfaces. Sections of the maximum, minimum, and average statistical surfaces, for $\|\dot{\omega}\| = 0$, are shown in Figure 3.

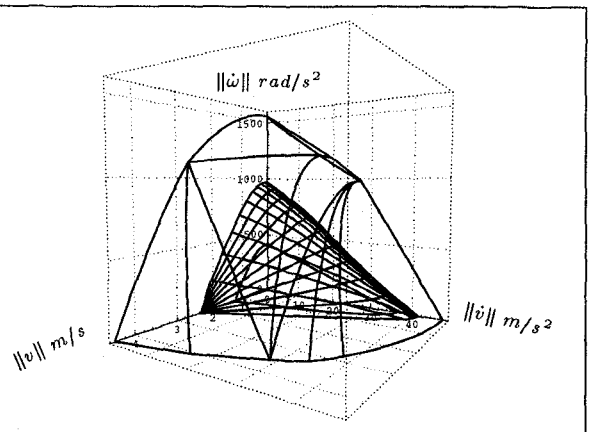

Figure 3: Surface Statistics.

3 Performance Measures

Several measures have been proposed as indicators for different characteristics related to dynamic performance. Rather than attempting to integrate all these different measures into one process, here an attempt is made to determine a measure which, to some extent, addresses each of those characteristics. This measure can then be used to formulate a simple cost function for an optimization procedure which has no arbitrary weighting factors upon which the solution will then be dependent.

The approach taken here is to determine a measure(s) which describes the effect of the Coriolis and centrifugal forces on acceleration capability. Examination of the Lagrangian dynamic formulation shows the relationship between the Coriolis/centrifugal forces and inertial properties of the mechanism. Briefly, a measure of these effects allows for design choices which reduce the Coriolis/centrifugal effects, (thereby increasing acceleration capability), and improve isotropy in the end effector inertial properties.

Performance measures are developed from the hypersurface characterization by determining the shape of the hypersurface for an ideal manipulator and measuring how close the actual is to the ideal hypersurface. Ideally Coriolis/centrifugal would be absent from the equations of motion since, in the worst case, they reduce acceleration capability once the manipulator begins to move. Although it is unclear what the relationship between linear and angular acceleration should be, it is assumed that ideally they would not be coupled. Thus the ideal hypersurface should appear as a rectangular hyperparallelipiped which extends out to infinity in the velocity directions.

However, unless Coriolis/centrifugal terms are completely absent, end effector velocities usually impose some limit on acceleration. Thus the ideal surface is defined as a rectangular hyperparallelipiped where the length of each side is determined by the intercepts of the actual hypersurface. A section of the ideal hypersurface is shown as the dashed lines forming the rectangular parallelipiped in Figure 2, (some of the connecting lines are omitted). The ideal surface is specified by giving the ratios of the lengths its sides,

$$\{\ \|\dot{v}_\times\|_{m/s^2}\ :\ \|\dot{\omega}_\times\|_{rad/s^2}\ :\ \|v_\times\|_{m/s}\ :\ \|\omega_\times\|_{rad/s}\ \}, \tag{7}$$

where the $\times$ subscript denotes the intercept value. Note that the size of ideal hypersurface changes along with the actual hypersurface at different configurations. In the example of Figure 2 the ideal surface specified as, $\{20.90 m/s^2 : 1336 rad/s^2 : 0.561 m/s : 10.35 rad/s\}$.

A measure relating the shapes of the actual and ideal hypersurfaces is obtained by determining how much the ideal surface must be proportionately reduced in order that its most distal corner touch the actual hypersurface. Computing the reduction involves assigning the vector corresponding to that corner a variable magnitude, β, and substituting its elements into equation (6). For example,

$$\beta\, \mathcal{A} \begin{bmatrix} \|\dot{v}_\times\| \\ \|\dot{\omega}_\times\| \end{bmatrix} + \beta^2\, \mathcal{C}\left(\|v_\times\|, \|\omega_\times\|\right) = \begin{bmatrix} \Upsilon_{upper} \\ \Upsilon_{lower} \end{bmatrix}, \tag{8}$$

where β is a dimensionless scalar. The smallest positive root from equation (8), expressed as a percentage, is chosen as the value for β. For the example of Figure 2 the percentage is $\beta = 36.39\%$.

This measure is highly dependent on the Coriolis/centrifugal approximation, $\mathcal{C}\left(\|v\|, \|\omega\|\right)$, in areas where, for the most general manipulator, it is not exact. However, the exact analytical solution for $\mathcal{C}\left(\|v\|, \|\omega\|\right)$ may be found for the three DOF planar mechanism. For the most general case, β can be determined numerically.

Another useful measure is obtained by proportionally reducing the ideal hypersurface until its most distal corner lying in the $\|\dot{v}\|$-$\|\dot{\omega}\|$ plane touches the curve of the actual hypersurface in that plane. This

measures the reduction of the ideal hypersurface in the absence of Coriolis/centrifugal forces. Computing the reduction is accomplished by considering only the isotropic accelerations in equation (6). For example,

$$\alpha \mathcal{A} \begin{bmatrix} \|\dot{v}_\times\| \\ \|\dot{\omega}_\times\| \end{bmatrix} = \begin{bmatrix} \Upsilon_{upper} \\ \Upsilon_{lower} \end{bmatrix}, \qquad (9)$$

where α is a dimensionless scalar. For the example of Figure 2 $\alpha = 73.70\%$.

The measure used in the optimization procedure, γ, is defined as,

$$\gamma = \frac{\alpha}{\beta}. \qquad (10)$$

This measure describes the reduction in acceleration capability caused by the Coriolis/centrifugal forces. Figure 4 shows sections of the two hyperparallelipipeds representing α and β in larger dashed lines. γ is actually the ratio of the size of these surfaces; $\gamma = 0.49$ for the example. If the Coriolis/centrifugal forces do not reduce acceleration capability the value of these measure may be greater than or equal to one. The measures become greater than one if the Coriolis/centrifugal forces help the mechanism achieve higher accelerations in every direction. At kinematic singularities $\gamma = 0$.

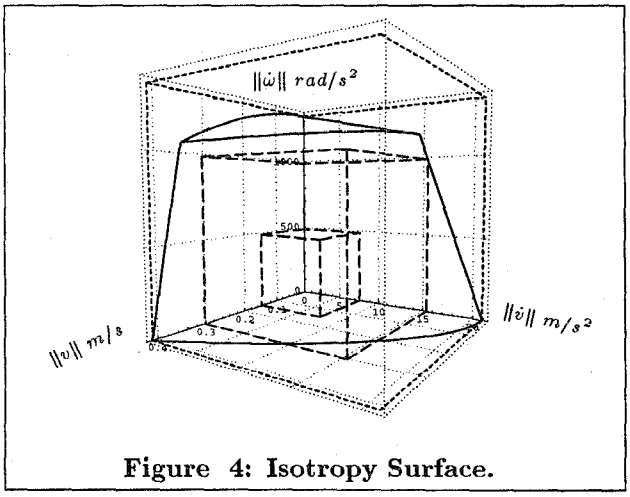

Figure 4: Isotropy Surface.

4 Design Methodology

The information contained in the hypersurface characterization and the measures obtained from it allow development of an optimization which simultaneously address several issues related to dynamic performance. Each of these issues is discussed in the following sections. Within this context the optimization scheme is also presented.

4.1 Performance and Actuator Sizing

Many studies propose different methods for characterizing and measuring dynamic performance. Yoshikawa [19, 21] developed the well known dynamic manipulability ellipsoid (DME). Our previous work in this area resulted in the acceleration parallelipiped [10]. Kim and Desa [11] developed acceleration set theory. Graettinger and Krogh [6] proposed the acceleration radius. In these studies the general approach is to transform actuator torque surfaces and/or joint velocities into acceleration surfaces. Isotropy in acceleration capability is usually measured by the condition number of the transformation matrix. Each study also proposes methods for determining the end effector isotropic acceleration based on their particular characterization.

A commonality between these studies is the recommendation that end effector acceleration capability should be made as isotropic as possible, both locally and over the workspace. The reasons for this include greater controllability due to the mechanism's increased ability to respond equally well to different controller commands. It is also desirable to increase the volume of the workspace within which different arbitrary commands can be executed equally well.

Unlike most other studies, in our method isotropic acceleration and velocity surfaces are mapped into actuator forces. This procedure yields a great deal of information from simpler computations. Using the resulting hypersurface, a high degree of isotropy in the end effector acceleration capability can be achieved, depending on the available actuators.

This can be accomplished to a certain extent simply by the choice of actuators. Note that given desired isotropic accelerations for a particular configuration, the actuators required to provide that level of performance can be determined iteratively using equation (6). Actuators are chosen to be just large enough to satisfy the desired performance level. This results in a high level of isotropy in acceleration capability. In this work the condition numbers of the mapping matrices E_v and, E_ω, from equation (4), are used to measure isotropy in acceleration capability.

The desired dynamic performance is an input to the design optimization. In this article the desired performance is expressed as the desired average ideal hypersurface for the workspace, equation (7). A list of possible actuator choices must also be provided.

4.2 Workspace Volume

Many studies have addressed the design and determination of a manipulator's reachable and dextrous

workspace, [7, 17, 18]. Our procedure assumes that the basic kinematic structure of the mechanism is predetermined. However, the optimization changes some of the design parameters and thus may ruin a carefully designed workspace by adding singularities or making some parts unreachable. The size of the workspace is maintained by adding constraints on the design parameters and the condition number of the jacobian at each configuration.

The condition of the workspace is maintained by the cost function. The cost function is defined as,

$$cost = (\bar{\gamma} - \sigma), \tag{11}$$

where $\bar{\gamma}$ and σ are the average and deviation of γ over a number of different configurations in the workspace.

As stated earlier γ is set equal to zero when the configuration is at a kinematic singularity and also for unreachable points. If the design parameters are changed such that significant portions of the workspace become unreachable or the altered workspace contains many singularities, the deviation, σ, will increase thus reducing the cost function. Therefore, the optimization will prefer mechanisms which maintain the workspace reflected in the choice of configurations.

4.3 Inertial properties

Asada [2] showed that achieving isotropy in the inertial properties, Λ, over the workspace decreased the size of the Coriolis/centrifugal terms in the equations of motion. The converse of this statement is also true. This is mainly due to the fact that the Coriolis/centrifugal forces are generated by changes in the inertial properties as a result of changes in the manipulator's configuration; as can be seen in the Lagrangian dynamic formulation [5]. A mechanism with isotropic end effector inertial properties is more amenable to interactions with humans since the the same inertial resistance is felt in every direction. However, this analysis did not address the inhomogeneities between the properties associated with linear and angular motion which are combined within Λ.

The inhomogeneity issue was addressed by the formulation of an effective mass matrix, Λ_v, and effective inertia matrix, Λ_ω, in [8]. However, it is difficult to determine whether achieving isotropy in these subspaces of the overall inertia matrix will decrease the Coriolis/centrifugal forces. The recommendation from this source is to achieve isotropic effective masses and inertias which are as small as possible in magnitude. These properties govern the natural behavior of the system and are especially important when the mechanism comes into contact with the environment since a controller cannot instantaneously respond to the forces generated at the instant of contact. Isotropy in mass and inertia can be measured using the condition numbers of Λ_v and Λ_ω. The norms of these matrices measure the magnitudes of those properties.

Maximizing $\bar{\gamma}$, or $\bar{\gamma} - \sigma$, decreases the nonlinear forces, however, it is difficult to know whether this will translate into isotropic effective masses and inertias. Theoretically this can be examined by considering the kinetic energy of the mechanism;

$$KE = \frac{1}{2} \begin{bmatrix} \dot{v}^T & \dot{\omega}^T \end{bmatrix} \Lambda \begin{bmatrix} \dot{v} \\ \dot{\omega} \end{bmatrix}. \tag{12}$$

The following transformation can be defined,

$$\begin{bmatrix} \dot{v} \\ \dot{\omega} \end{bmatrix} = \Lambda^{-1} \begin{bmatrix} \dot{\tilde{v}} \\ \dot{\tilde{\omega}} \end{bmatrix}, \tag{13}$$

where $\dot{\tilde{v}}$ and $\dot{\tilde{\omega}}$ are considered to be inverse effective velocities and,

$$\Lambda^{-1} = \begin{bmatrix} \Lambda_v^{-1} & \Lambda_{v\omega}^{-1} \\ \Lambda_{v\omega}^{-T} & \Lambda_\omega \end{bmatrix}. \tag{14}$$

Using equation (13) in equation (12) yields,

$$KE = \dot{\tilde{v}}^T \Lambda_v^{-1} \dot{\tilde{v}} + \dot{\tilde{\omega}}^T \Lambda_\omega^{-1} \dot{\tilde{\omega}} + 2\dot{\tilde{v}}^T \Lambda_{v\omega}^{-1} \dot{\tilde{\omega}}. \tag{15}$$

The analysis presented in [2] can be applied to the first two terms in equation (15) to show how isotropy in Λ_v^{-1} and Λ_ω^{-1} reduces the Coriolis/centrifugal forces, but it is unclear how the coupling term will affect this conclusion. However, it may be impossible to achieve isotropy in the overall Λ due to the inhomogeneity between the mass and inertia, both present in Λ. Therefore, some reduction in Coriolis/centrifugal forces can be obtained by achieving isotropy in the effective mass and effective inertia properties, again, depending on the coupling terms.

4.4 Controllability

As stated above, γ measures the effect of Coriolis/centrifugal forces on acceleration capability. Maximizing γ reduces the effects of these forces so that higher isotropic accelerations can be achieved while the mechanism is in motion. In addition to these benefits, reducing the Coriolis/centrifugal effects makes detailed modeling of these terms less critical for some control schemes. For instance, the computed torque method [5], which relies on the linearization of the system model by subtracting out the nonlinearities.

In our earlier optimization studies the choice of weightings for the different components of the cost

function determined the compromise between improving the mechanism's inertial and acceleration properties. Here, this compromise is governed by improvement of the acceleration properties which in turn should improve the inertial properties.

4.5 Optimization Procedure

The NPSOL software program for nonlinear programming, developed by the Systems Optimization Laboratory at Stanford University, was used to facilitate the search of the design parameter space. The details required to implement this software, other than the cost function, will not be discussed here. However, the capability of expressing nonlinear as well as linear constraints in the formulation is a benefit. This allows the desired performance to be expressed as a nonlinear constraint. Therefore the actuators can be considered as design parameters to be optimized.

The procedure for optimizing the design involves first minimizing the size of the actuators required to provide the desired performance. The cost function for this first optimization is simply the sum of the actuator capacities. The result from this initial stage is then used as a constraint on the sum of the actuators for the Coriolis/centrifugal effects reduction. The cost function for this stage of the optimization is given in equation (11). The results from this stage are then used as a constraint on the desired cost to be maintained for the actuator capacity minimization step. These two stages are repeated until a satisfactory result is obtained.

5 Application

In this section presents the application of the optimization procedure to the three DOF planar manipulator with three revolute joints shown in Figure 1. The following discussion is framed by addressing the issues discussed in section 4. The design parameters consist of the three link lengths, L_1, L_2, and L_3, subject to the constraint, $8\ cm \geq L_i \geq 50\ cm$. In this case the desired performance, specified as the average ideal hypersurface for the workspace, is $\{43\ m/s^2\ :\ 720\ rad/s^2\ :\ 1.7\ m/s\ :\ 24\ rad/s\}$.

For the sake of comparison, the actuators computed for the final design are used for the initial design. As expected, the choice of actuators makes the linear acceleration capability of the final design highly isotropic; the average condition number of E_v, and its deviation over the workspace are $\kappa(E_v) = 1.8 \pm .38$. For the initial design $\kappa(E_v) = 2.1 \pm .48$. The end effector of the planar manipulator has only one rotational DOF thus $\kappa(E_\omega) = 1$ always.

In order to maintain the workspace volume a constraint was enforced requiring a minimum total extension of 38 cm for the three links. The manipulator was also optimized for 240 configurations. Three fourths of the configuration set is generated by discretizing the range of each joint and generating all permutations of those sets of joint angles. One fourth of the configurations are generated using inverse kinematics to determine joint angles corresponding to particular points in the workspace.

The initial and final design parameters are given in Table 2 along with the averages and deviations for the performance measures over the workspace. First notice the increase in the overall size of the mechanism from initial to final design. The optimization did increase $\bar{\gamma}$ by 8.5% over the initial design, although σ increased slightly. Thus the overall effect of the Coriolis/centrifugal forces on acceleration capability was reduced.

	Initial	Final
L_1	17 cm	26 cm
L_2	17 cm	23 cm
L_3	14 cm	8 cm
extension	48 cm	57 cm
α	52 ± 3.3	51 ± 2.1
β	36 ± 3.4	37 ± 3.9
$(\bar{\gamma} - \sigma)$	$0.7 - 0.064$	$0.76 - 0.07$

Table 2. Initial versus Final Design

Evidence of this reduction is shown in Figures 5 and 6 and their accompanying average ideal surface specifications. These figures show sections of the maximum, minimum, and average statistical surfaces. Note that the final design, Figure 6 can perform arbitrary motions at higher velocities than the initial design. Also notice in Figure 5 that the initial design does not provide the desired performance.

The effective mass and inertia properties can be examined to see if the process behaved as expected. Table 3 summarizes the measures for the average inertial properties along with their deviations. Note that although the final design is overall a larger manipulator than the initial design, it still has comparable inertial properties. The final design shows an almost four-fold improvement in the effective inertia, $Norm(\Lambda_v)$. The average effective mass, $Norm(\Lambda_v)$, is slightly smaller in the final design than in the initial and varies less over the workspace. However, the effective masses in the initial design are slightly more isotropic than in the final design.

It is interesting to note that the average condition number of overall inertia matrix, $\kappa(\Lambda)$, increased from the initial to the final design. These results support

the idea that maximizing $\bar{\gamma} - \sigma$ separately improves isotropy in the effective mass and inertia properties.

$\{ 59 \pm 8 : 695 \pm 191 : 2.7 \pm 0.9 : 25 \pm 13 \}$

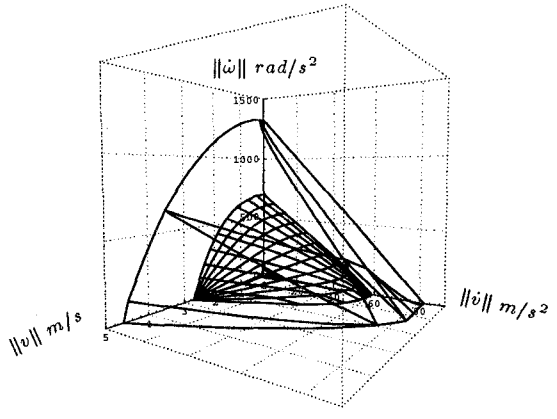

Figure 5: Initial Design Performance.

$\{ 47 \pm 6 : 817 \pm 197 : 3 \pm 0.8 : 37 \pm 15 \}$

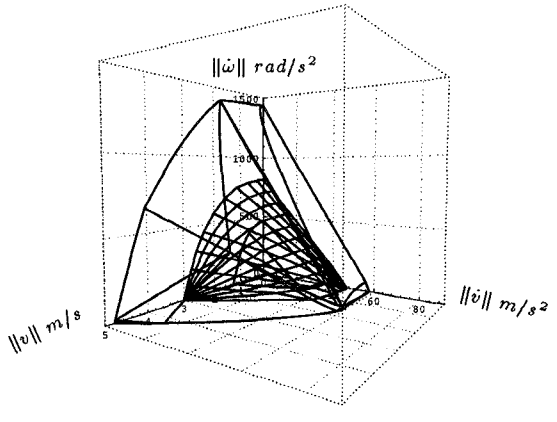

Figure 6: Final Design Performance.

	Initial	Final
$\kappa(\Lambda_v)$	9.5 ± 4.5	9.8 ± 4.7
$Norm(\Lambda_v)\ kg$	0.33 ± 0.16	0.32 ± 0.15
$Norm(\Lambda_\omega)\ kgm^2$	$6e^{-4} \pm 4e^{-5}$	$2e^{-4} \pm 6e^{-6}$
$\kappa(\Lambda)$	2076	3381

Table 3. Inertial Properties.

The initial design in this study is a fairly good design. It is interesting to note that the use of the proposed procedure, with it's simple cost function, maintained the good characteristics of the initial design but improved the design where possible.

6 Conclusion

We have presented a general methodology for designing manipulators for a high level of dynamic performance. This methodology makes use of new performance measures developed from a characterization of acceleration capability which we recently introduced. The new measure allows formulation of an optimization problem with a simple cost function having no arbitrary weights or scaling factors to determine. This optimization was shown to address several issues related to design for dynamic performance while providing a manipulator capable of providing the desired performance. The process was illustrated on a three DOF planar manipulator.

Acknowledgments

The financial support of NASA/JPL, General Motors, and NSF, grant IRI-9320017, are gratefully acknowledged.

References

[1] J. Angeles. The design of isotropic manipulator architectures in the presence of redundancies. *The International Journal of Robotics Research*, 11(3):196–201, June 1992.

[2] H. Asada. Dynamic analysis and design of robot manipulators using inertia ellipsoids. In *Proceedings of the IEEE International Conference on Robotics*, March 1984. Atlanta, Georgia.

[3] A. Bowling. *Analysis of Robotic Manipulator Dynamic Performance: Acceleration Capability.* PhD thesis, Stanford University, 1997. Soon to be published.

[4] A. Bowling and O. Khatib. Analysis of the acceleration characteristics of non-redundant manipulators. In *Proceedings IEEE/RSJ International Conference on Intelligent Robots and Systems*, volume 2, pages 323–328. IEEE Computer Society Press, August 1995. Pittsburgh, Pennsylvania.

[5] J. J. Craig. *Introduction to Robotics: Mechanics and Control.* Addison-Wesley Publishing Company, second edition, 1989.

[6] T. J. Graettinger and B. H. Krogh. The acceleration radius: A global performance measure for robotic manipulators. *IEEE Journal of Robotics and Automation*, 4(1), February 1988.

[7] K. C. Gupta and B. Roth. Design considerations for manipulator workspace. *Journal of Mechanical Design: Transactions of the ASME*, 104(4):704–711, October 1982.

[8] O. Khatib. Inertial properties in robotic manipulation: An object-level framework. *The International Journal of Robotics Research*, 13(1):19–36, February 1995.

[9] O. Khatib and S. Agrawal. Isotropic and uniform inertial and acceleration characteristics: Issues in the design of redundant manipulators. In *Proceedings of the IUTAM/IFAC Symposium on Dynamics of Controlled Mechanical Systems*, 1989. Zurich, Switzerland.

[10] O. Khatib and J. Burdick. Optimization of dynamics in manipulator design: The operational space formulation. *The International Journal of Robotics and Automation*, 2(2):90–98, 1987.

[11] Y. Kim and S. Desa. The definition, determination, and characterization of acceleration sets for spatial manipulators. *The International Journal of Robotics Research*, 12(6):572–587, 1993.

[12] C. A. Klein and B. E. Blaho. Dexterity measures for the design and control of kinematically redundant manipulators. *The International Journal of Robotics Research*, 6(2):72–83, 1987.

[13] K. Kosuge and K. Furuta. Kinematic and dynamic analysis of robot arm. In *Proceedings IEEE International Conference on Robotics and Automation*, volume 2, 1985.

[14] R. V. Mayorga, B. Ressa, and A. K. C. Wong. A kinematic design optimization of robot manipulators. In *Proceedings IEEE International Conference on Robotics and Automation*, volume 1, 1992.

[15] F. C. Park and R. W. Brockett. Kinematic dexterity of robot mechanisms. *The International Journal of Robotics Research*, 13(1):1–15, 1994.

[16] J. K. Salisbury and J. J. Craig. Articulated hands: Force control and kinematic issues. *The International Journal of Robotics Research*, 1(1):4–17, 1982.

[17] R. Vijaykumar, K. J. Waldron, and M. J. Tsai. Geometric optimization of serial chain manipulator structures for working volume and dexterity. *The International Journal of Robotics Research*, 5(2):91–103, 1986.

[18] D. C. H. Yang and Z. C. Lai. On the dexterity of robotic manipulators-service angle. *Journal of Mechanisms, Transmissions, and Automation in Design: Transactions of the ASME*, 107:262–270, 1985.

[19] T. Yoshikawa. Dynamic manipulability of articulated robot arms. In *15th International Symposium on Industrial Robots*, September 1985.

[20] T. Yoshikawa. Manipulability of robotic mechanisms. *The International Journal of Robotics Research*, 4(2), 1985.

[21] T. Yoshikawa. Translational and rotational manipulability of robotic manipulators. In *Proceedings of the 1991 International Conference Industrial Electronics, Control, and Instrumentation*, October 1991.